Challenge Journal of Concrete Research Letters

Research Article

Assessment of stresses and vibration behavior of concrete gravity dam under fluctuating hydrostatic force

Pandimani [a,*]

[a] *GMR Institute of Technology, Rajam, Vizianagaram District, 532127 Andhra Pradesh, India*

ABSTRACT

Dam structure contributes to the socio-economic development of a country but zero probability of failure of such structure is a design concern. Hence, it is essential to monitor the dam condition under the fluctuating reservoir water and the vibration effect. In this investigation, four different cases of the reservoir depths are adopted to numerically analyze the hydrostatic and modal (free-vibration) behavior of a three-dimensional (3D) gravity dam. The impact of fluctuating reservoir water and uplift pressure on the dam's internal stresses (direct, principal, shear, and Von Mises) are evaluated to examine the location of maximum stress concentration. Under these cases, the maximum displacement along the longitudinal and vertical directions is explored. It can be revealed that case 1 (with full reservoir) induces the maximum displacement on the top crest level and the peak normal stress concentrated at the heel region, respectively. The mode shapes 1 and 4, under case 4 reveals the peak and lowest time-period. Whereas, the frequency responses are in contrast to it (i.e., reverse) under the same case and modes. In comparison to cases 2, 3, and 4, case 1 exhibit the largest crest level displacements along the x-direction that are 26%, 49%, and 86% higher, respectively. Compared to case 1, the normal stresses along the x-direction declined by 51.58%, 68.74%, and 58.25%, respectively for cases 2, 3, and 4. It can be revealed that the frequency is directly related, while the time-period is inversely proportional to the mode-shapes. Overall, this study envisages a comprehensive understanding of the dam's performance, providing critical data to inform design decisions, safety assessments, and performance improvements.

ARTICLE INFO

Article history:
Received – July 16, 2024
Revision requested – September 14, 2024
Revision received – September 18, 2024
Accepted – September 26, 2024

Keywords:
Stress analysis
3D modeling
Dam-reservoir structure
Time-period
Frequency
Mode shapes

Citation: Pandimani (2025). Assessment of stresses and vibration behavior of concrete gravity dam under fluctuating hydrostatic force. *Challenge Journal of Concrete Research Letters*, 16(1), 1–14.

1. Introduction

In water resource management, structural integrity is essential to ensure the safety and longevity of water-retaining structures like gravity dams. The significant challenge for ensuring the safety of such structures relies on the fluctuating reservoir and uplift pressure effect, which compromise the stability and durability of a dam. Understanding the effect of these forces is crucial for improving the dam's performance and ensuring its structural safety. It is also essential to understand the dynamic effect, which causes severe damage to the dam structure due to the vibration. The mode shape and frequency behavior of the dam structure is a critical parameter that essentially provides valuable insights into the structural performance of the dam. It also assists engineers in predicting the potential weaknesses within the dam body and optimizing the design for durability and safety concerns. Understanding the causes and mechanisms of the structural deformation process is essential for the safety of man-made dam structures, for protecting the environment, and for the establishment of associated mitigating measures in the event of natural disasters. The impounding reservoir of a dam can cause natu-

* *Corresponding author*. Tel.: +91-89191-17823 ; E-mail address: pandimani918@gmail.com (Pandimani)
ISSN: 2548-0928 / DOI: https://doi.org/10.20528/cjcrl.2025.01.001

ral tragedies like earthquakes and the sudden collapsing of such a structure would cause severe devastation of property and human life. The environmental consequences of dam construction would have direct impacts on the physical, biological, and chemical features of rivers and riparian environments. In recent years, the evolution of vibration damage and the impact of impounding reservoir pressure have become major concerns for the safety and serviceability of dams. Reservoir and dam construction involves substantial anthropogenic and natural impacts. They are mostly positive effects but sometimes it influences the negative impact on the environment. The main purpose of dam construction involves the improvement of the local water regime which consequently enhances the national prosperity. The socioeconomic developments of the country by generating power, irrigation of cultivated land, municipal water supply, navigation, and flood control are the main goals of constructing the reservoir and dam. However, the consequences of dam construction have also some negative environmental impacts such as migration of local people, drastic changes in the reservoir's aquatic life, and natural hazards, which cannot be avoided. The structure of a solid gravity dam can be built with concrete or stone masonry material constructed to form the backwater reservoir. The lateral reservoir pressure is primarily resisted by the weight of the dam. The dam considered in this study is a multi-purpose irrigation project that is under construction across the River Godavari, located in the districts of West and East Godavari of Andhra Pradesh.

A comparative study between two and three-dimensional arch dams (gravity-type) were performed considering earth and reservoir pressure influence on the longitudinal displacement. The reservoir depth was 6.2m lowered and the effect of displacements on the crest level was investigated. It was demonstrated that both three and two-dimensional studies correlated closely with the experimental tests (Žvanut 2022). Two-dimensional static responses under fluctuating reservoir levels considering the dam structure and soil interaction were investigated through the ANSYS package. It was demonstrated that the highest crest displacement was achieved for a flexible foundation compared to a rigid one. It was inferred that beyond 2H width and 1.5H depth of foundation, the dam stresses are insignificant on the foundation-structure interaction effect (Sharma and Nallasivam 2023). A two-dimensional high-gravity dam was analyzed under 0.1 g to 0.3 g lateral ground motion to investigate the stability and stress conditions. It was concluded that the stability of the dam has been endangered by increasing earthquake intensity. It was suggested that the numerical shear and vertical stress magnitudes are more conservative than the gravity method (Ali et al. 2012). To investigate the safety measures of the dam under seismic forces, a finite element approach was employed using the domain reduction method and free-field boundary condition methods and the stresses and displacements results are compared. Later the domain reduction method was employed considering the foundation as rigid, mass, and massless for the Koyna dam. It was revealed that the dam responses are overestimated for the massless foundation type (Ghaemian et al. 2019). An appropriate finite element method (free-field boundary condition) using ABAQUS was implemented considering the effects of radiation damping, mass, and wave propagation. The responses of the foundation-dam effect assuming mass and massless were evaluated. It was illustrated that the foundation with massless assumption overestimates the magnitude of stresses and displacements (Mohammadnezhad et al. 2019). Earthquake analysis was done numerically using a case study of Koyna dam for the dam-structure interaction effect and the results are validated with past literature. A foundation with mass was assumed and the damage indices, crack evolution, displacements, and principal stresses were evaluated. The simulated result specifies that the massed foundation has a significant influence on the seismic performance of the gravity dam (Burman et al. 2008). A parametric numerical analysis was performed to explore the impact of the flexibility and rigidity foundations type on the free vibration frequency characteristics of the dam. The dam was also studied with and without the prestress effect. It was predicted that the dam with initial prestress would exhibit more frequency than that without prestressing case. It was also suggested that the initial condition and boundary conditions should be considered while assessing the dam responses under the foundation-dam interaction effect (Jafari and Khiavi 2019). A 2D roller compacted concrete dam was analyzed for dynamic responses to examine the effect of the shape and size of the gallery using the ABAQUS package. It was demonstrated that the circular shape gallery performed better regarding stress concentration, deflection, and crack formation, compared to the octagonal and square shapes (Ghaedi et al. 2016). A numerical study was executed to extract the responses of the dam structure foundation interaction assuming rigid and flexible boundaries. A numerical study was further extended to investigate the optimum depth and width of the foundation. It was concluded as related to the fixed base type, the flexible (considering foundation) base produced 10 times higher deflection. It was examined that the optimum foundation width of twice the dam height and optimum depth of 1.5 times the height of the dam was achieved (Abraham et al. 2017). Modal analysis of the gravity dam was numerically simulated considering different reservoir and tail-water levels and the effect of reservoir-foundation-dam interactions. It was concluded that the highest lateral deformation occurred under lower reservoir depth. The higher reservoir height with tail-water height offers more flexibility and reduced frequency. In contrast to the interaction between reservoir water and dam structure, the interaction between the reservoir water, dam, and foundation combination produces lesser frequency (Tidke and Adhikary 2022).

This paper highlights the 3D reservoir pressure modeling and stresses analysis of the Polavaram project gravity dam profile, which is rarely presented in the past literature. The study explores the impact of varying the u/s, uplift, and d/s water forces to investigate the peak stress concentration and displacement region within the dam. Excessive stresses within the dam can lead to a cracking or failure of concrete material, which compromises the integrity of the structure. Engineers can iden-

tify the potential zone of weakness that may require reinforcement or design adjustments to prevent any catastrophic failure. Excessive displacements can potentially lead to the overturning and sliding of dams, hence monitoring the displacement behavior under fluctuating reservoir forces ensures the dam remains within safe operating limits. It also evaluates the vibration behavior to examine the natural frequency and mode shape parameters to assess the potential weakness area inside the body of the dam. It is possible to optimize the dam geometry and materials consumption by accurately predicting the peak stresses and displacement parameters before the commencement of dam construction. It also ensures the dam structure is resilient to both static and dynamic loadings. The presented model can be adopted as a reference to examine the influence of other significant factors on dam stability and its responses to external forces, which is a future scope of this study.

2. Gravity Dam Modeling

The Indian government designated the Polavaram dam project a significant undertaking in Andhra Pradesh, as a national project (Amarnath and Shashidhar 2020). It is situated in the Godavari River and is regarded as the region's most important infrastructure undertaking. It is a multi-use dam that is being built for irrigation and hydroelectric power, and it has the potential to be the largest dam in India. The non-overflow sectional view of the dam is shown in Fig. 1, which depicts the various parameters concerning the dam. In this section, a 3D gravity dam is analyzed using STAAD Pro V8i package. The dam is studied for 4 different u/s reservoirs and tailwater depths, to assess the critical regions of displacements and stresses within the body of the dam.

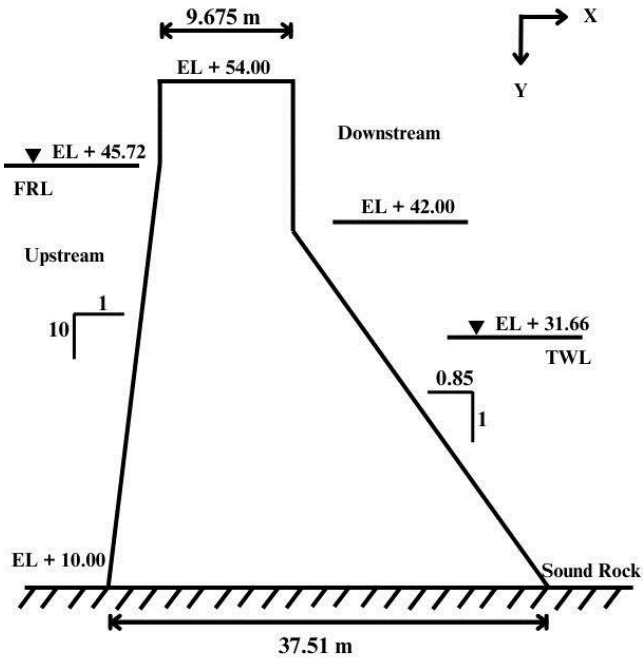

Fig. 1. Sectional view of the gravity dam (Amarnath and Shashidhar 2020).

The non-overflow section is 54m high, 9.675m in top width, and 37.51m in bottom width. In this study, the 3D structure of a dam of 20m in length is assumed for analysis purposes. From the base, an inclination of 10:1 up to a height of 35.72m and then vertically upward till the top crest level on the upstream (u/s) side. It has a downstream (d/s) slope of 1:0.85 up to a height of 32m and then vertically upward till the top crest level of the dam. A water depth of 21.66m is avail on the downstream side with a Full Reservoir Level (FRL) of 35.72m available on the upstream side respectively (with a dam base lying at RL of +10m). STAAD Pro, commercial version is an extensively employed design and structural analysis software developed by Research Engineers International (STAAD Pro 2007). Later in 2005, it was bought by Bentley Systems. It is capable of modeling structural steel, timber, cement concrete, and other composite structural elements with design codes of several nations. It is capable of performing, various geometric and material linear as well as nonlinear static and dynamic analyses. In STAAD Pro, three basic methods are available for developing the geometry of the structure such as the snap node method, coordinate method, and copy-paste method. It also consists of a few default structural models in its command wizard library for frames, solids, and truss-type structures. In this study, a default cuboid solid model is used to generate a 3D dam structure by the coordinate system method in the STAAD editor. The research methodology employed to perform this analysis work is represented in Fig. 2.

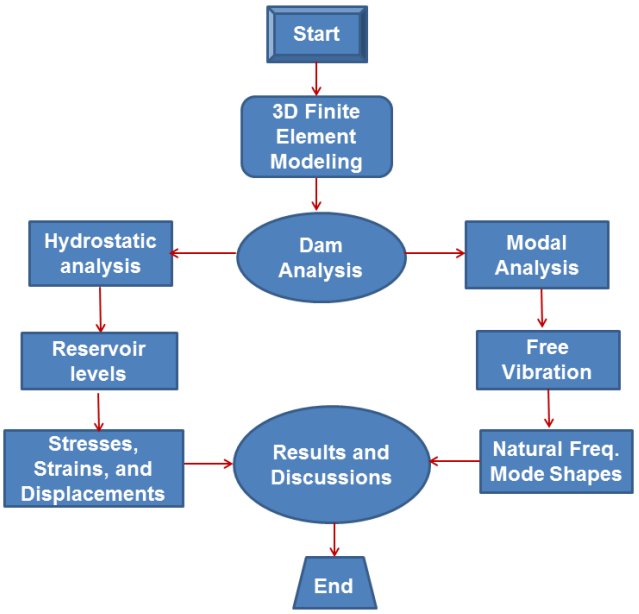

Fig. 2. Methodology used for dam analysis in STAAD Pro.

Unlike shell (plate) elements and members, solid elements do not require any attributes. However, constants such as the Poisson's ratio and elasticity modulus must be given. In addition, density needs to be provided in each load case where self-weight is included. Solid elements enable the solution of structural problems with general three-dimensional stresses. A powerful tool for solid components finite element analysis is offered for a

class of problems, including the distribution of stress in rock and soil strata or concrete dams. In this study, an eight-node, isoparametric solid element is employed to develop the dam model using STAAD Pro. Each node of this solid element has freedom in three translational directions, and the geometry shape is illustrated in Fig. 3.

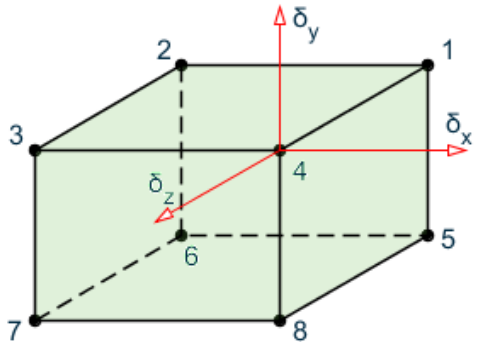

Fig. 3. Eight-node isoparametric element (STAAD Pro 2007).

It is likely to impose uniform and linearly varying pressure on the faces of the solid element through the solid load tab. On a face, a volumetric type of pressure is applied, where the intensity at one node may differ from another node within the same face. This kind of load is defined by the water weight on a dam's sloping face. If the dam is represented with solids for each component, the water height at the lower elevation nodes will be higher than those at the higher elevation nodes. The pressure can be applied in the local z-direction (normal to the element) or the global directions (i.e., x, y, and z). If we neglect the global orientation, we assume that the applied loading is normal to the face and that a positive pressure is entering the solid. At the four corner nodes of the dam section, the boundary conditions at supports are given zero displacements and rotations (fixed) in the translational directions (i.e., x, y, and z). To perform the static and modal analysis, the self-weight of the dam is input by assigning linear elastic material properties (i.e., Density and Poisson's ratio) of concrete (Pandimani et al. 2023a, 2023b). Table 1 illustrates the geometric details of the dam-reservoir structure. Table 2 represents the modulus of elasticity, Poisson's ratio, weight density, and damping ratio values that are employed in this study. The concrete grade of M35 is assumed for the 3D solid model.

Among various studied cases: Case 1: 35.72 m of reservoir water level and 21.66 m of tailwater, Case 2: 30.72 m of reservoir water level and 17.66 m of tailwater, Case 3: 25.72 m of reservoir water level and 13.66 m of tailwater, and Case 4: 35.72 m of reservoir water level with no tail-water, are the various cases assumed for the dam's analysis. The dam's dead load (self-weight), pressure due to uplift, downstream water pressure, and upstream hydrostatic pressure are the forces exerted on the dam's surface (FRL). 35.72 meters is the reservoir's upstream depth, and 21.66 meters is the highest tail-water level. A non-overflow section of the dam has a height of 44 meters. The rock foundation of the non-overflow section is available at an elevation of 10m. The top and bottom widths are 9.675m and 37.51m respectively. On the u/s and d/s sides of the dam, there is a slope of one horizontal to ten vertical and 0.85 horizontal to one vertical, respectively. The analysis assumes a 20-meter length for the dam.

Table 1. Dam-reservoir data considered.

S.No.	Parameters	Value
1	Full Reservoir depth	35.72 m
2	Maximum depth of tail water	21.66 m
3	Height of the dam	44.00 m
4	Sound rock level	10.00 m
5	Width of the dam at the bottom	37.51 m
6	Width of the dam at the top	9.675 m
7	Length of the dam considered	20.00 m
8	Upstream slope	1H:10V
9	Downstream slope	0.85H:1V

Table 2. Material properties.

S.No.	Particulars	Type/Value
1	Type of material	Concrete
2	Type of element	Solid 8-node quadrilateral
3	Young's modulus of concrete (E_c)	29580.39 N/mm^2
4	Density of concrete (D_c)	2.5 E-5 N/mm^3
5	Density of water	9810 N/m^3
6	Poisson's ratio (PRXY)	0.30
7	Damping ratio (DAMP)	0.05
8	Concrete grade	M35

3. Hydrostatic Reservoir Loadings

The solid loading diagrams for various reservoir water levels at the upstream, downstream, and uplift faces are shown in this section. As shown in Fig. 4, three forces: upstream reservoir thrust, uplift pressure, and downstream tail-water pressure are modeled as solid volume pressures acting on the corresponding faces of 3D solid elements. Throughout the length (20m) of a gravity dam, a trapezoidal (for cases 1-3) and triangular (for case 4) volumetric uplift pressure (varying load) is acting at the dam's bottom face. Whereas a varying triangle volumetric pressure is acting at the upstream and downstream faces of the dam respectively.

This study uses four case studies, as shown in Fig. 4(a-d), to determine the static and modal responses. For the first case, the water level in the u/s and d/s is 35.72m and 21.66m respectively. The reservoir depth or the second case are 30.72m u/s and 17.66m d/s respectively. The third case has water levels of 25.72m and 13.66m u/s and d/s respectively. In the last scenario, the reservoir depth is 35.72 meters on the u/s side, and there is no tail-water in the d/s face. The water level in the u/s and d/s faces affected the uplift pressure in each of the four examples. The volumetric pressure (solid hydrostatic) exerted on the different regions of the dam is shown by the green and blue colored diagram in Fig. 4.

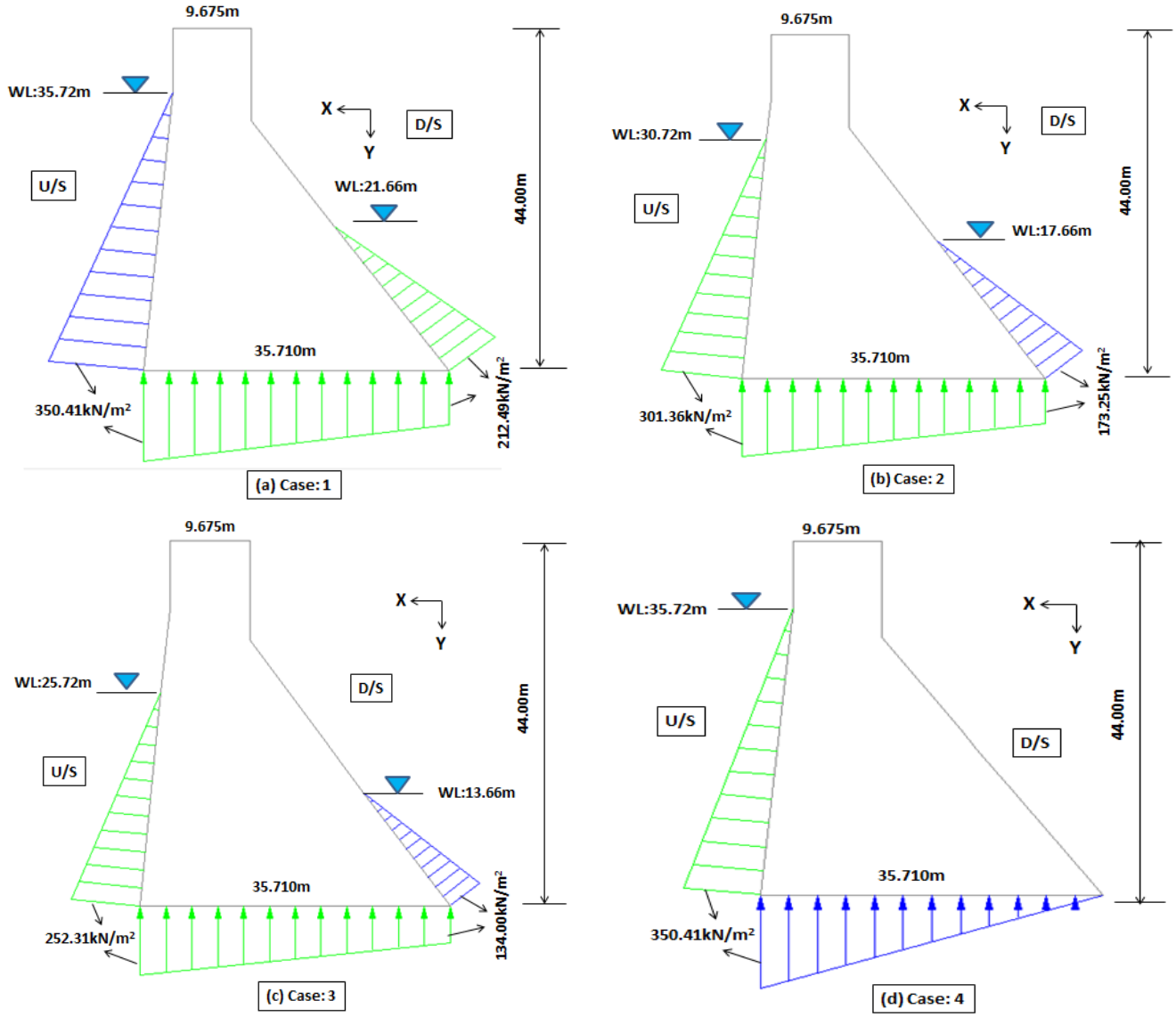

Fig. 4. Hydrostatic pressure loading diagram: (a) Case 1; (b) Case 2; (c) Case 3; (d) Case 4.

The theoretical formula presented in Eqs. (1) to (4) are employed to compute the pressure magnitudes at upstream, tail-water, and uplift, respectively (Punmia et al. 2009). The evaluated theoretical pressure intensities under various studied cases are presented in the subsequent section below.

The u/s reservoir pressure at dam base:

$$P_{(u/s)} = \gamma_w \cdot h_1 \quad (1)$$

The d/s pressure due to tail water at dam base:

$$P_{(d/s)} = \gamma_w \cdot h_2 \quad (2)$$

Uplift pressure at dam base (u/s):

$$P_{u1} = \gamma_w \cdot h_1 \quad (3)$$

Uplift pressure at dam base (d/s):

$$P_{u2} = \gamma_w \cdot h_2 \quad (4)$$

where, h_1 = u/s side height of reservoir (m); h_2 = d/s side tail-water height (m); γ_w = density of water (kN/m^3).

4. Results and Discussion

This section includes the proposed 3D solid gravity dam's graphical representation and analysis of the results under different reservoir depths and tail-water water levels. Additionally, modal behavior and the free vibration effect are illustrated. The results of solid loading are discussed, and visual representations of the stress analyses under various loading conditions and their variations in stresses are provided. Additionally, graphs illustrating how natural frequency varies under different mode shapes are displayed.

4.1. Stress analysis

Demonstrates the various case studies employed in this study to investigate the impact of fluctuating reservoir pressure exerting over the dam body. The responses like direct stress, von-Mises stress, shear stress, and principal stresses are extracted numerically and the results are interpreted comprehensively.

Table 3. Details of the hydrostatic loading cases.

S.No.	Particular details	Case-1	Case-2	Case-3	Case-4
1	Height of reservoir in the upstream (h_1), m	35.72	30.72	25.72	35.72
2	Height of tail-water in the downstream (h_2), m	21.66	17.66	13.66	0
3	Density of water (γ_w), kN/m^3	9.81	9.81	9.81	9.81
4	Reservoir u/s pressure at the top, kN/m^2	0	0	0	0
5	Reservoir u/s pressure at the bottom, kN/m^2	350.42	301.36	252.31	350.42
6	Uplift pressure in the upstream face, kN/m^2	350.42	301.36	252.31	350.42
7	Uplift pressure in the downstream face, kN/m^2	212.48	173.24	134.00	0
8	Pressure on the d/s face at the top due to tailwater, kN/m^2	0	0	0	0
9	Pressure on d/s face at the bottom due to tailwater, kN/m^2	212.48	173.24	134	0

4.1.1. Case study 1

In this case, the elevation of the u/s reservoir and tail-water is at 35.72m (FRL) and 21.66m respectively as shown in Fig. 4(a). A u/s reservoir pressure of 0 kN/m^2 atmospheric pressure and 350.420 kN/m^2 at the dam's heel portion was applied. Similarly, uplift pressures of 350.420 kN/m^2 and 212.48 kN/m^2 were applied on the dam heel and toe region respectively. A 0 kN/m^2 and 212.480 kN/m^2 were assigned at the 21.66m level (atmospheric) and toe of the dam as tail water pressure. Maximum normal stresses of magnitudes 285 kN/m^2 (comp.), 105 kN/m^2 (tensile), 147 kN/m^2 (comp.), and 147 kN/m^2 (tensile) are predicted along the x- and y-direction respectively, as illustrated in Table 5. The maximum displacement of 616.987 mm and 188.759 mm is produced along the x- and y-directions as presented in Table 4, which occurs at the dam's top crest region.

The largest and lowest von-Mises stress and principal stress of 376 kN/m^2 (comp.), 52.3 kN/m^2 (comp.) and 164 kN/m^2 (comp.), 1.13 kN/m^2 (tensile) are developed under case 1, as presented in Table 6. The dam's heel region exhibits the highest direct stress along the x-direction, whereas the u/s side of the dam experiences the highest normal stress in the y-direction respectively, as revealed in Fig. 5(a-b). The largest and lowest von-Mises contour stresses, which are concentrated at a dam's mid-height on the u/s side and top crest, respectively, are shown in Fig. 5(c). The findings indicate that, as depicted in Fig. 5(d), the top head region and the d/s side of the dam are where the least principal stress forms, and the largest principal stress occurs at the u/s face.

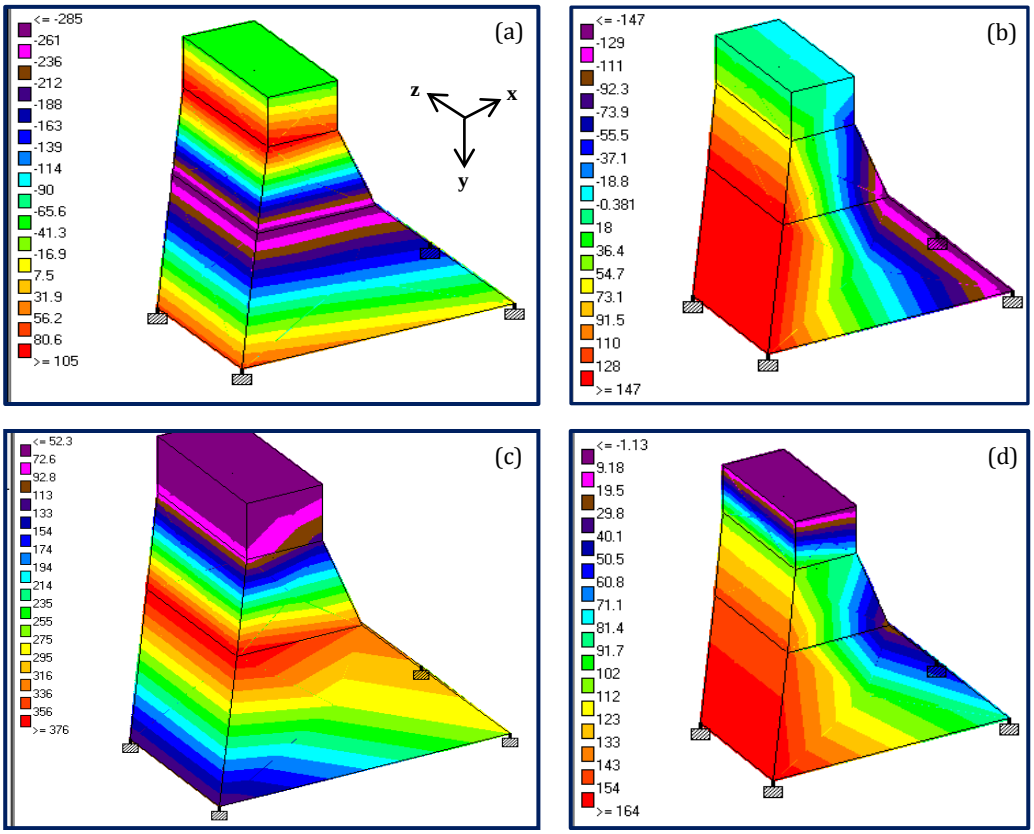

Fig. 5. Contour stress diagrams for case 1:
(a) Normal stress in x-direction; (b) Normal stress in y-direction; (c) von-Misses stress; (d) Principal stress.

4.1.2. Case study 2

As seen in Fig. 4(b), the level of the u/s water and tail-water in this case are at 30.72 m and 17.66 m, respectively. On the u/s side, a reservoir pressure of 0 kN/m² (atmospheric pressure) and 301.360 kN/m² were applied at the dam's heel region. Similarly, the uplift pressure at the dam toe and heel portion was 173.240 kN/m² and 301.360 kN/m², respectively. A tail-water pressure of 0 kN/m² and 173.240 kN/m² is assigned at 17.66m height and dam toe portion, respectively. Fig. 6(a-b) show the predicted highest and least normal stresses along the x- and y-directions, respectively. The magnitudes of these stresses are 138 kN/m² (comp.), 40.9 MPa (tensile), 126 kN/m² (comp.), and 96 kN/m² (tensile), respectively.

The highest crest level of the dam developed a maximum displacement of 456.208 mm (x-dir.) and 299.092 mm (y-dir.), as shown in Table 4. The largest and lowest von-Mises and principal stresses of 207 kN/m² (tensile), 19.9 kN/m² (tensile), and 98.2 kN/m² (tensile), 1.13 kN/m² (tensile) are developed under case 2. The highest and lowest von-Mises stresses develop at the top reservoir level on the u/s face and top crest region of the dam respectively, as shown in Fig. 6(c). It was revealed that the largest principal stress developed at the u/s side and the lowest principal stress formed at the top head region on the d/s side of the dam, as shown in Fig. 6(d). The normal stresses along the x- and y-directions are maximum on the u/s face and minimum on the d/s face of the dam respectively and illustrated in Fig. 6(a-b). Tables 5 and 6 illustrate the predicted stress results of normal, von-Mises, and principal stresses respectively.

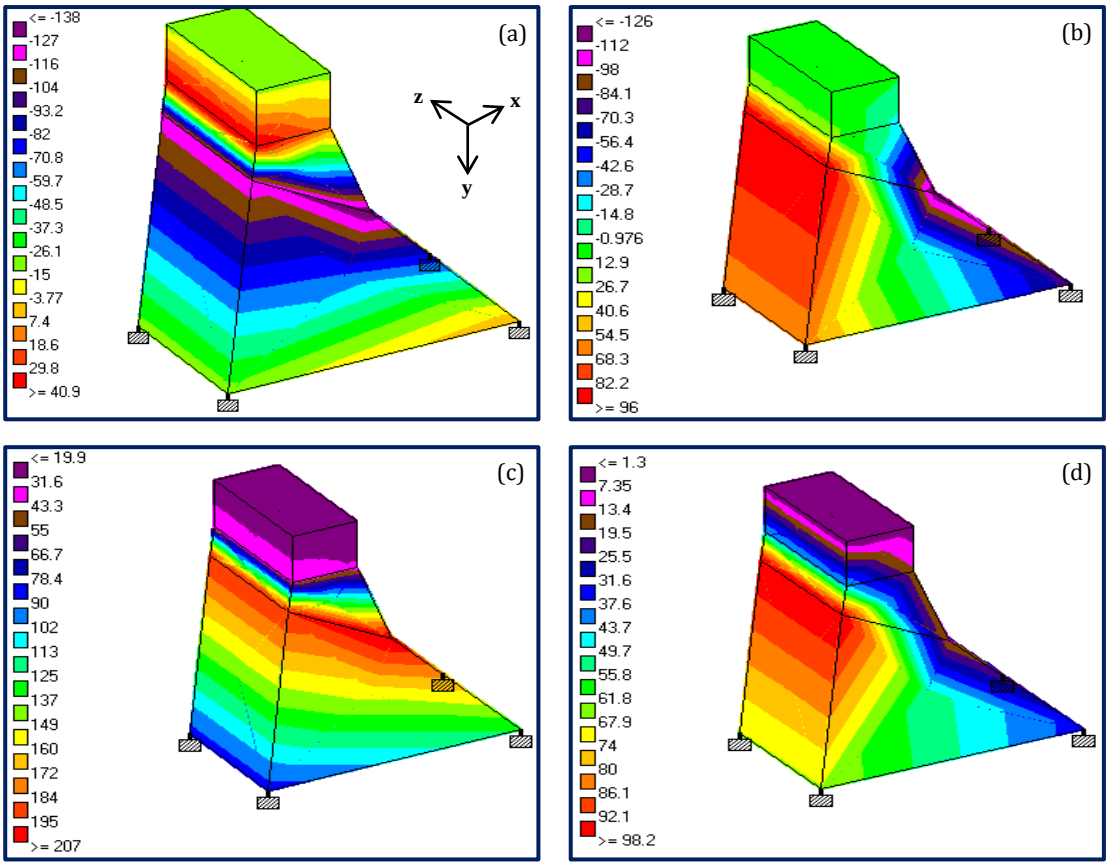

Fig. 6. Contour stress diagrams for case 2:
(a) Normal stress in x-direction; (b) Normal stress in y-direction; (c) von-Misses stress; (d) Principal stress.

4.1.3. Case study 3

As seen in Fig. 4(c), the levels of the u/s water and tail-water in this case are 25.72 m and 13.66 m, respectively. On the u/s side, a reservoir pressure of 0 kN/m² (atmospheric pressure) and 252.310 kN/m² were applied at the dam's heel region. Likewise, the uplift pressure at the dam toe and heel was 134 kN/m² and 252.310 kN/m², respectively. A tail-water pressure of 0 kN/m² and 134 kN/m² were assigned at the 16.66m level and toe of the dam. As displayed in Fig. 7(a) and (b), maximum normal stresses of magnitude 89.1 kN/m² (comp.), 42.2 kN/m² (tensile), and 61.8 kN/m² (tensile), 77 kN/m² (comp.) are anticipated along the x- and y-directions, respectively.

Table 4 illustrates the maximum displacement of 311.859 mm and 87.97 mm was developed at the top crest region of the dam. Under case 3, the von-Mises and principal stresses of maximum and minimum magnitudes of 129 kN/m² (tension), 26.30 kN/m² (tension), and 67 kN/m² (comp.), 0.047 kN/m² (comp.), are developed. Fig. 7(c) illustrates the maximum and minimum von-Mises stresses that are concentrated at the top reservoir level and top crest portion of the dam respectively, on the u/s side. It is investigated that, as indicated

in Fig. 7(d), the least principal stress develops at the top head region and d/s face of the dam respectively. Furthermore, the largest principal stress concentrated on the u/s face. The largest and lowest normal stresses are developed on the dam's u/s and d/s faces along the x- and y-directions, respectively.

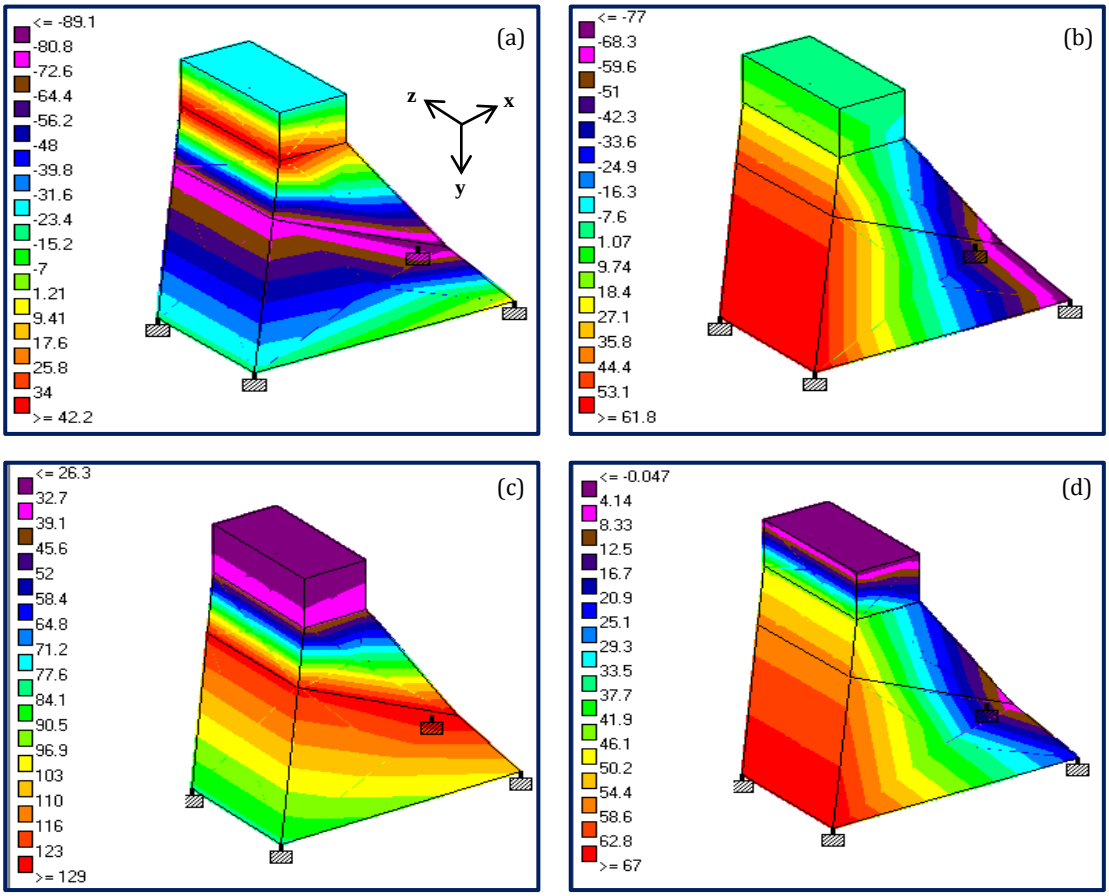

Fig. 7. Contour stress diagrams for case 3:
(a) Normal stress in x-direction; (b) Normal stress in y-direction; (c) von-Misses stress; (d) Principal stress.

4.1.4. Case study 4

As seen in Fig. 4(d), in this case, the height of the u/s levels is 35.72m (FRL.) with no tail-water. On the u/s side, a reservoir pressure of 0 kN/m^2 (atmospheric pressure) and 350.420 kN/m^2 were applied at the dam's heel region. Similarly, the uplift pressure at the dam toe and heel was set at 0 kN/m^2 and 350.420 kN/m^2, respectively. As displayed in Fig. 8(a) and (b), the maximum normal stresses of magnitudes 119 kN/m^2 (comp.), 12.8 kN/m^2 (comp.), and 222 kN/m^2 (comp.), 217 kN/m^2 (tensile), are anticipated along the x- and y-directions, respectively.

Tables 5 and 6 illustrate the predicted stress magnitudes of normal, von Mises, and principal stresses respectively. Table 4 illustrates the maximum displacement of 1369.199 mm and 395.058 mm was developed at the top crest level of the dam. The largest and lowest von-Mises and principal stresses of 321 kN/m^2 (tensile), 62.9 kN/m^2 (tensile) and 222 kN/m^2 (tensile), 14.60 kN/m^2 (comp.) are developed under case 4. The concentrations of the highest and minimum von-Mises stresses are developed at the d/s face and top head region of the dam respectively, as displayed in Fig. 8(c). As seen in Fig. 8(d), it was revealed that the lowest principal stress forms at the top crest region and d/s edge of the dam, whereas the largest principal stress forms at the u/s face.

4.2. Displacements

Table 4 illustrates the highest displacements along the x- and y-directions of a 3D gravity dam influenced by fluctuating levels of hydrostatic pressures. According to cases 1 through 4, the greatest displacements of magnitude 616.987 mm, 456.208 mm, 311.859 mm, and 87.970 mm in the x-direction and 188.759 mm, 299.092 mm, 369.199 mm, and 395.058 mm along the y-direction are anticipated. Table 4 and Fig. 9, illustrate that the maximum displacements in the x-direction descents as the reservoir depth lowers, but in contrast, this magnitude increases in the y-direction when the reservoir levels decrease. Fig. 9 shows that the greatest displacements in the x- and y-directions of 616.978 mm and 395.058 mm, respectively. In comparison to cases 2, 3, and 4, case 1 has displacements in the x-direction that are 26%, 49%, and 86% higher, respectively. Conversely, the greatest displacements under case 1 are 58%, 96%, and 109% smaller than those under cases 2, 3, and 4, respectively in the y-direction. It is determined that the dam's crest region is subjected to the largest displacements along the x- and y-directions, respectively.

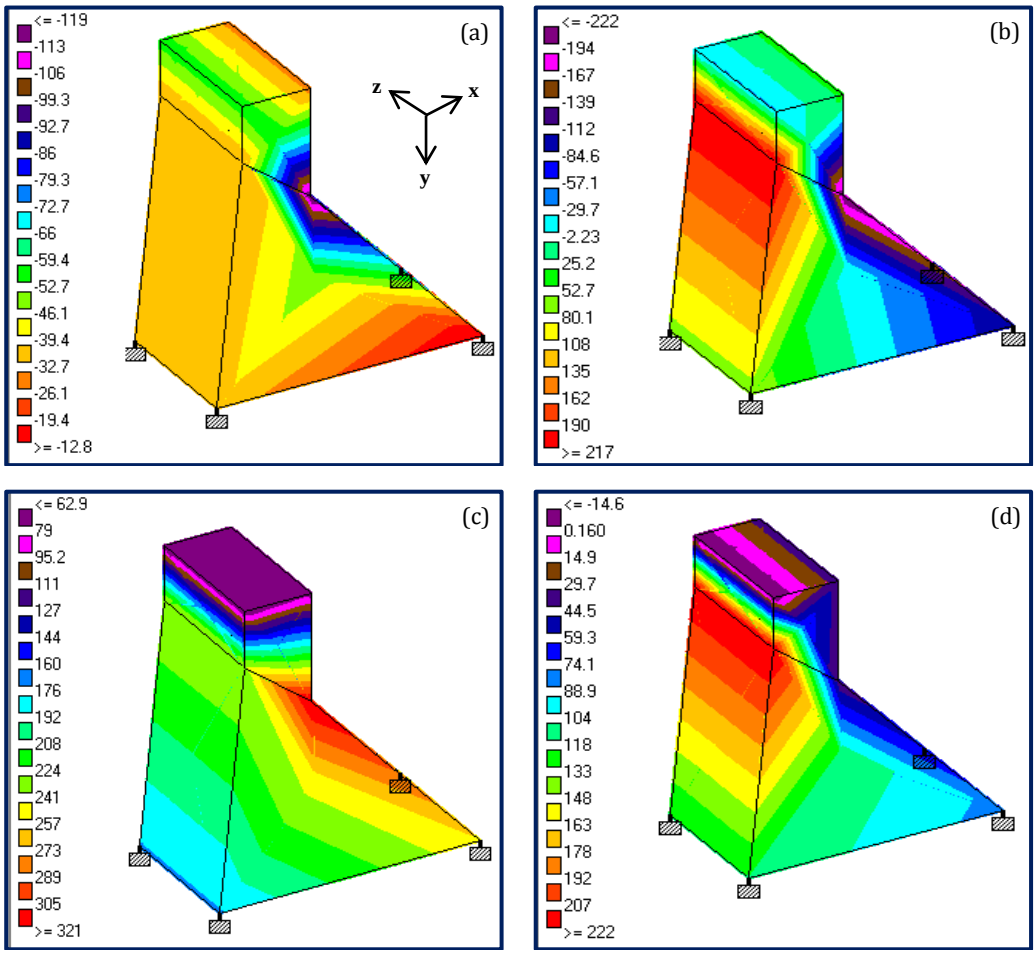

Fig. 8. Contour stress diagrams for case 4:
(a) Normal stress in x-direction; (b) Normal stress in y-direction; (c) von-Misses stress; (d) Principal stress.

Table 4. Maximum predicted displacements (mm).

Direction	Case 1	Case 2	Case 3	Case 4
x-	616.987	456.208	311.859	87.970
y-	188.759	299.092	369.199	395.058

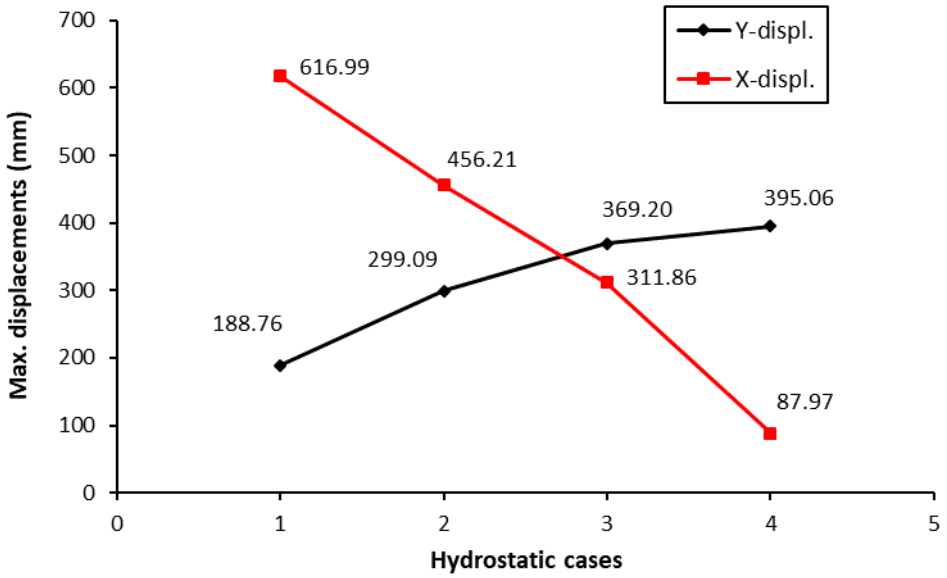

Fig. 9. Maximum node displacements along x- and y-directions.

4.3. Normal (direct) stress

Table 5 shows the expected maximum and minimum normal stress magnitudes along the x- and y-directions under the variable reservoir depths. As shown in Fig. 10, cases 1 through 4 cause maximum compressive stresses of magnitudes 285 kN/m², 138 kN/m², 89.10 kN/m², and 119 kN/m², respectively. It is observed that along the x-direction, every produced stress has a compressive nature. Similarly, as illustrated in Fig. 10, the highest stresses of magnitudes 147 kN/m², 126 kN/m², 61.80 kN/m², and 222 kN/m² were assessed for cases 1 through 4, respectively, along the y-direction. All other cases have compressive stresses in the y-direction, except case 3. Compared to case 1, the normal stresses in the x-direction for cases 2, 3, and 4 declined by 51.58%, 68.74%, and 58.25%.

Table 5. Maximum and minimum normal stresses (kN/m²).

Direction	Case1		Case 2		Case 3		Case 4	
	max	min	max	min	max	min	max	min
x-	-285	+105	-138	+40.9	-89.1	+42.2	-119	-12.8
y-	-147	+147	-126	+96	+61.8	-77	-222	+217

Note: (-) sign indicates compressive and (+) indicates tensile stresses.

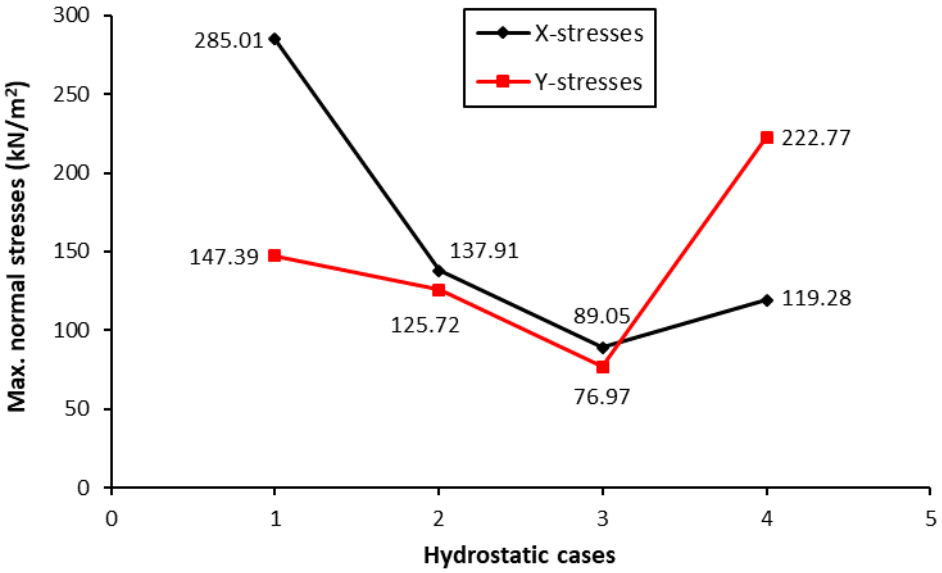

Fig. 10. Maximum normal stresses along x- and y-directions.

4.4. von-Mises and principal stresses

Table 6 displays the highest and lowest von-Mises and principal stresses for cases 1 to 4. The maximum von-Mises and principal stresses are depicted in Fig. 11. The maximum von-Mises stress of 376 kN/m² and 222 kN/m² are predicted under cases 1 and 4 respectively. In comparison to case 1, the maximum von-Mises stresses for cases 2, 3, and 4 are reduced by 44.95%, 65.70%, and 14.63%, respectively. Similar reductions of 40.12% and 59.15% are seen in the maximum principal stresses of cases 2 and 3, while a 35.37% rise is seen in case 4 relative to case 1. It is revealed that under the four different cases studied, all the principal stresses are tensile. It is examined that the maximum von-Mises stresses for case 1 is 14.63% higher than that of case 4, which reveals that it is 1.17 times that of case 4. In comparison to case 4, the maximum principal stress in case 1 decreased by 35.37%, indicating that it is 0.74 times greater than that of case 4.

Table 6. von-Mises and principal stresses (kN/m²).

	Case-1		Case-2		Case-3		Case-4	
	max	min	max	min	max	min	max	min
von-Mises stress	376	52.3	207	19.9	129	26.3	321	62.9
Principal stress	+164	-1.13	+98	+1.3	+67	-0.04	+222	-14.6

Note: (-) sign indicates compressive and (+) indicates tensile stresses.

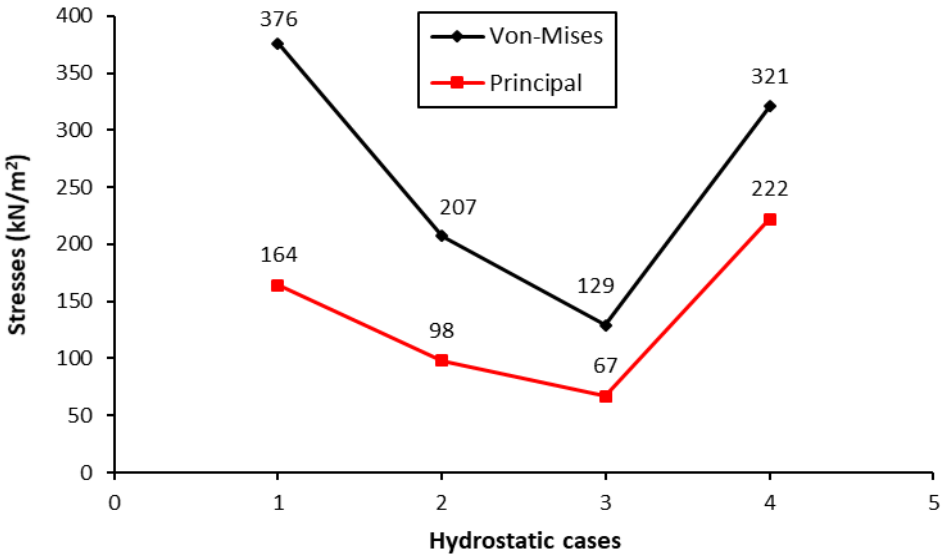

Fig. 11. Maximum von-Mises and principal stresses.

4.5. Shear stresses

Table 7 displays the maximum shear stresses in the x- and y-directions for various loading cases. It is revealed that case 4 develops the largest shear stresses. In the x-direction, the maximum shear stresses for cases 1 through 4 are, in order, 141.60 kN/m², 85.63 kN/m², 54.83 kN/m², and 135.42 kN/m² respectively. The highest shear stress magnitudes of 13.51 kN/m², 7.09 kN/m², 3.57 kN/m², and 19.08 kN/m² are recorded for cases 1 through 4, respectively, along the y-direction. It is investigated along the x-direction and found that, in comparison to case 1, case 2 offers a percentage reduction in maximum shear stress of 39.53. Similarly, in the x-direction, case 3 shows a percentage reduction in maximum shear stress of 35.97 and 61.28, respectively, when compared to cases 2 and 1. In comparison to case 1, case 4 exhibits an x-direction percentage reduction of 4.36 of the maximum shear stress. Conversely, for case 4, the maximum shear stress decreased by 58.15% and 146.98% along the x-direction respectively, when compared to cases 2 and 3.

Table 7. Maximum shear stresses (kN/m²).

Case	x-dir.	y-dir.
1	141.60	13.51
2	85.63	7.09
3	54.83	3.57
4	135.42	19.08

Furthermore, a comparison of cases 2 and 3 against case 1 along the y-direction reveals a reduction of maximum shear stress of 47.52 and 73.25 percent, respectively. In comparison to case 2, case 3 also yields a 49.65% reduction in shear stress. In contrast, the largest shear stress for case 4 in the y-direction is increased by 41.23%, 169.11%, and 434.45% compared to cases 1, 2, and 3, respectively.

4.6. Modal analysis

A method for determining the vibration specifications of the dam structure can be assessed using modal (frequency) analysis (Punmia et al. 2009; Asghari et al. 2018; Pandimani et al. 2023b). The vibration of any structure like dams can be made with force or without force and can generally be described as forced or free vibrations. Under free vibrations, the structure may oscillate at specific natural frequencies and periods, and the respective deformation is referred to as mode shape (Wang et al. 2021; Li et al. 2015; Khosravi and Heydari 2015).

The modal analysis is executed to establish the time-period, natural frequency, and respective mode shapes, which offers crucial information about the structure responses before the more realistic dynamic analysis (Punmia et al. 2009; Pandimani et al. 2023a, 2023b). Free vibration analysis is performed to extract the mode shape, time-period, and natural frequency (Hz) for the 4 solid models executed in this study. Fig.12 reveals that the natural frequency increases with the mode shape, i.e., the higher the mode number higher the frequency for all the cases. Fig.13(a-d) represent the different mode shapes from cases 1 to 4 respectively. Table 8 depicts the predicted natural frequencies and time periods under the studied cases.

Among the various cases and mode shapes, case 4 (without tail water pressure) under the fourth mode exhibits the highest natural frequency, as shown in Fig. 12. The highest time-period existed for case 1 under mode-4 and the least time-period for case 4 under mode-4 respectively, as shown in Table 8 and Fig.14. The variation of time-period under various modes of vibration is presented in Fig. 14. The natural frequency ranges from 0.571Hz to 1.503Hz for case 1, 0.660Hz to 2.819Hz for case 2, 1.062Hz to 3.733Hz for case 3, and 0.518Hz to 19.627Hz for case 4. It was concluded that the natural frequencies of mode number 4 in cases 1, 2, 3, and 4 are 2.63, 4.27, 3.52, and 37.88 times that of the first mode respectively. It is clear from Table 8 that the frequencies under the first mode increased by 15.59% for case 2

compared to case 1. The frequency is increased by 60.91% and 85.99% for case 3 in comparison to case 2 and case 1 respectively, for mode 1. In contrast, the frequency under case 4 declined by 9.28%, 21.52%, and 51.22% against the case 1, 2, and 3 respectively. Similarly, the mode 2 frequency under cases 2 and 3 are increased by 28.86% and 96.88% respectively, against case 1. Whereas, a 48.43% increase in frequency is achieved for case 3 in comparison to case 2. The frequency for the second mode under case 4 is increased by 6.70% and decreased by 17.19%, and 45.80% in comparison to cases 1, 2, and 3 respectively.

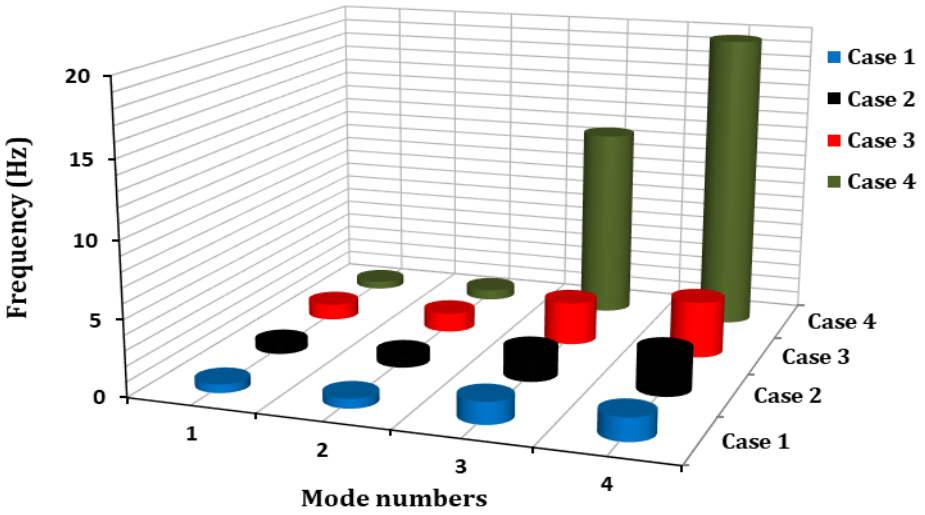

Fig. 12. Comparison of natural frequency.

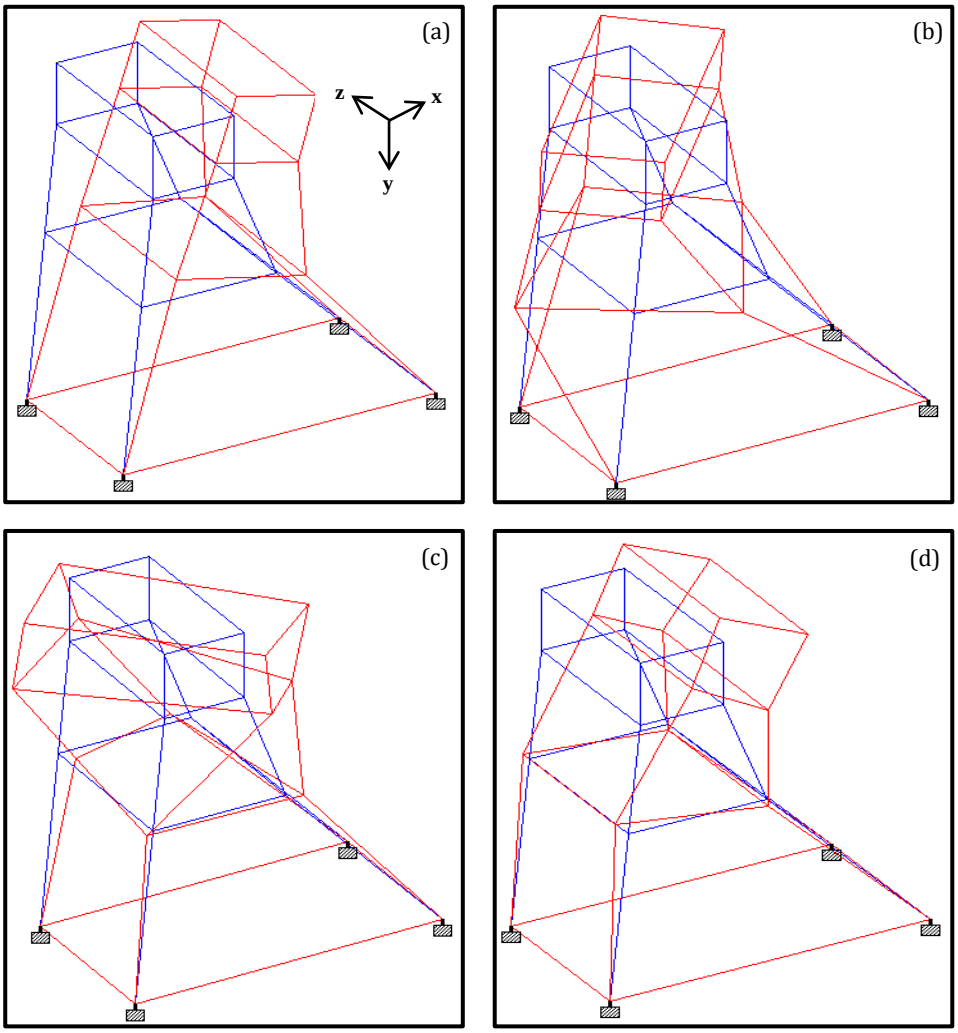

Fig. 13. Mode shapes of the dam section:
(a) Mode shape 1; (b) Mode shape 2; (c) Mode shape 3; (d) Mode shape 4.

Table 8. Modal analysis responses (free vibration).

Modes	Frequency (Hz)				Period (seconds)			
	Case-1	Case-2	Case-3	Case-4	Case-1	Case-2	Case-3	Case-4
1	0.571	0.660	1.062	0.518	1.752	1.516	0.941	1.932
2	0.641	0.826	1.262	0.684	1.561	1.210	0.793	1.462
3	1.448	1.968	2.842	12.620	0.691	0.508	0.352	0.079
4	1.503	2.819	3.733	19.627	0.665	0.355	0.268	0.051

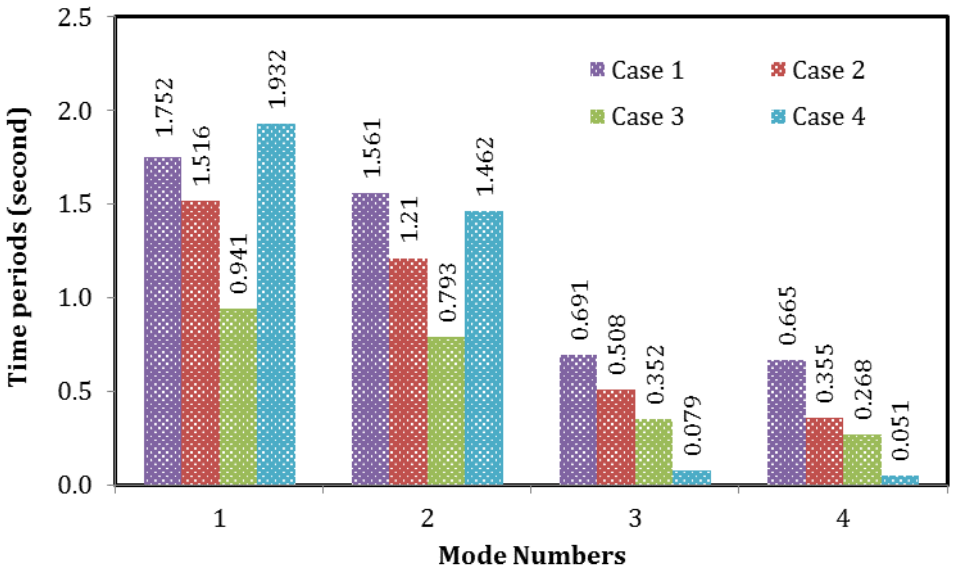

Fig. 14. Comparisons of time-periods.

Compared to case 1, the mode 3 frequency is increased by 35.91% and 96.27% for cases 2 and 3 respectively. Whereas, a 44.41% increased frequency is achieved for case 3 against case 2. A large variation in the frequency was experienced under the fourth mode in case 4 related to the other cases due to zero tail water pressure, as depicted in Table 8 and Fig. 12. An 88.56% and 148.37% increase in frequency are observed for case 2 and 3 respectively, in comparison to the case 1. Similarly, a 33.43% increase in frequency is exhibited for case 3 against case 2. Similarly, Compared to frequencies of cases 1, 2, and 3 for mode number 4, the highest percentage increments of 1205.85, 596.24, and 425.77 are obtained under case 4.

5. Conclusions

This study encompasses the 3D analysis of a solid gravity dam which demonstrates that the dam's static and vibration responses may be satisfactorily anticipated using the advanced structural analysis and design software (STAAD Pro) tool. The expected results are deemed significant, and the package's robustness through contour graphical representation and user-friendly environment offers a better comprehension of the dam responses. The major vibration properties (such as mode shape and vibration frequencies) of the dam structure are investigated through modal analysis. The critical observations of this research are illustrated below.

- The largest displacement for case 1 in the x-direction is increased by 85.74% compared to case 4, which reveals that it is 7.01 times more than that of case 4. On the other hand, the maximum displacement under case 1 decreased by 109.29% compared to case 4, meaning that it is 0.48 times larger in the y-direction than case 4.
- Cases 1 and 4 exhibit the largest normal stresses respectively, along the x- and y-directions. It is determined that, in comparison to case 4, case 1 achieves a 58.25% increase in normal stress along the x-direction. Furthermore, under case 1, a declining percentage of 51.02 is shown in the y-direction in comparison to case 4. It can be concluded that the induced tensile and compressive stresses are within the limiting strength of the materials.
- The von-Mises stresses in case 1 are found to be 1.82, 2.91, and 1.17 times greater than those in cases 2, 3, and 4, correspondingly. The primary stresses in cases 1, 2, 3, and 4 were found to be 1.67, 2.45, and 0.74 times greater, respectively. In case 1, the maximum shear stresses show 41.23% lower and 4.36% greater along the x- and y-directions, respectively, compared to case 4.
- It is demonstrated that the natural frequencies and time-periods increased with increasing mode numbers. It is revealed through modal analysis (under free vibration) that the maximum and minimum frequencies are predicted in case 4, under mode 4 and mode 1 respectively. As opposed to this, case 4 discloses the

maximum and minimum time-periods under modes 1 and 4, respectively.

The combination of a full reservoir with tail-water makes the dam more flexible, which consequently lowers the natural frequency. Conversely, in modal analysis, a reservoir with lower water depth leads to increased lateral crest deformation. A dam with a full reservoir and tail water results in a lower natural frequency than a dam without tail-water.

Acknowledgements

None declared.

Funding

The author received no financial support for the research, authorship, and/or publication of this manuscript.

Conflict of Interest

The author declared no potential conflicts of interest with respect to the research, authorship, and/or publication of this manuscript.

Data Availability

The datasets created and/or analyzed during the current study are not publicly available, but are available from the corresponding author upon reasonable request.

REFERENCES

Abraham M, Kuriakose B, Kuruvilla R (2017). Static analysis of gravity dams considering foundation-structure interaction. *Applied Mechanics and Materials*, 857, 237-242.

Ali MH, Alam MR, Haque MN, Alam MJ (2012). Comparison of design and analysis of concrete gravity dam. *Natural Resources*, 3(1), 31004.

Amarnath CR, Shashidhar T (2020). Study on backwater effect due to Polavaram Dam Project under different return periods. *Water,* 12(2), 576.

Asghari E, Taghipour R, Bozorgnasab M, Moosavi M (2018). Seismic analysis of concrete gravity dams considering foundation mass effect. *KSCE Journal of Civil Engineering*, 22, 4988-4996.

Burman A, Reddy BV, Maity D (2008). Seismic analysis of concrete gravity dams considering foundation flexibility and nonlinearity. *The 12th International Conference of International Association for Computer Methods and Advances in Geomechanics*, Goa, India.

Ghaedi K, Jameel M, Ibrahim Z, Khanzaei P (2016). Seismic analysis of Roller Compacted Concrete (RCC) dams considering effect of sizes and shapes of galleries. *KSCE Journal of Civil Engineering*, 20, 261-272.

Ghaemian M, Noorzad A, Mohammadnezhad H (2019). Assessment of foundation mass and earthquake input mechanism effect on dam–reservoir–foundation system response. *International Journal of Civil Engineering,* 17, 473-480.

Jafari SR, Khiavi P (2019). Parametric study of the modal behavior of concrete gravity dam by using finite element method. *Civil Engineering Journal*, 5(12), 2614-2625.

Khosravi S, Heydari MM (2015). Design and modal analysis of gravity dams by ANSYS parametric design language. *Walailak Journal of Science and Technology*, 12(2), 167-180.

Li M C, Guo XY, Shi J, Zhu ZB (2015). Seepage and stress analysis of anti-seepage structures constructed with different concrete materials in an RCC gravity dam. *Water Science and Engineering*, 8(4), 326-334.

Mohammadnezhad H, Ghaemian M, Noorzad A (2019). Seismic analysis of dam-foundation-reservoir system including the effects of foundation mass and radiation damping. *Earthquake Engineering and Engineering Vibration*, 18, 203-218.

Pandimani, Rao YD, Krishna IG (2024). FE modeling for ultimate behavior predictions of RC beam. *Asian Journal of Civil Engineering*, 25(1), 477-493.

Pandimani, Sankar TS, Priyatham BPRVS, Ramkumar BAV (2024). Evaluation of SSI impact on the structural performance of RC buildings. *Asian Journal of Civil Engineering*, 25(2), 1295-1307.

Punmia BC, Lal PBB, Jain AK, Jain AK (2009). Irrigation and Water Power Engineering. Laxmi Publications, Ltd., India.

Sharma A, Nallasivam K (2023). Static analysis of a concrete gravity dam using the finite element technique. *Asian Journal of Civil Engineering*, 24(8), 2939-2957.

STAAD Pro (2007). Technical reference manual. Research Engineers, a Bentley Solutions Center. www.bentley.com/staad.

Tidke AR, Adhikary S (2022). Vibration characteristics of gravity dams for varying reservoir and tailwater heights, and interaction effects. In *Symposium in Earthquake Engineering,* Singapore: Springer Nature Singapore, 171-180.

Wang C, Zhang H, Zhang Y, Guo L, Wang Y, Thira Htun TT (2021). Influences on the seismic response of a gravity dam with different foundation and reservoir modeling assumptions. *Water*, 13(21), 3072.

Žvanut P (2022). 3D finite element analysis of a concrete dam behavior under changing hydrostatic load: A case study. *Materials*, 15(3), 921.